

# INFLUENCE OF CR-FREE ANTI-FINGERPRINT PASSIVATION FILMS ON THE FRICTION RESISTANCE OF HOT-DIP Al-Zn COATED CARBON STEEL SHEETS

## VPLIV TRENJSKE ODPORNOSTI PREVLEK BREZ KROMA ZA PASIVACIJO PROTI PRSTNIM ODTISOM NA JEKLENIH PLOČEVINAH PREVLEČENIH Z Al-Zn PREVLEKO, IZDELANIMI Z GLOBOKIM POTAPLJANJEM

Degao Qiao<sup>1</sup>, Jian Li<sup>1</sup>, Xingchang Tang<sup>2</sup>, Yongjing Shi<sup>3</sup>, Yi Wang<sup>2</sup>, Youzhi Cao<sup>2</sup>, Zhengqian Zhang<sup>2</sup>, Yang Li<sup>2</sup>, Deyi Zhang<sup>2\*</sup>

<sup>1</sup>Gansu Jiu Gang Group Hongxing Iron and Steel Co., Ltd., Gansu 73500, China

<sup>2</sup>State Key Laboratory of Advanced Processing and Recycling of Nonferrous Metals, Lanzhou University of Technology, Lanzhou 730050, China

<sup>3</sup>Department of Materials Science and Engineering, Chongqing University of Science and Technology, Chongqing 401331, China

*Prejem rokopisa – received: 2025-02-14; sprejem za objavo – accepted for publication: 2025-10-07*

doi:10.17222/mit.2025.1392

Currently, the absence of an effective scientific methodology for evaluating the friction resistance of Cr-free anti-fingerprint Al-Zn coated carbon steel sheets has significantly hindered the qualitative assessment and real-time monitoring of product quality by manufacturers and their downstream users. In this study, we systematically investigate the friction resistance of Al-Zn coated carbon steel sheets treated with three mainstream types of Cr-free anti-fingerprint passivation solutions: polymer-based (Granocoat 621), silane-based (DS981LX), and resin-based (PC-815) passivation solutions, utilizing a high-speed ring-block friction and wear tester. Our experimental results reveal that the friction coefficient curves exhibit a distinct three-stage pattern, corresponding to the sequential wear of the passivation film, the Al-Zn alloy layer, and the underlying carbon steel substrate. Notably, the initial significant increase in the friction coefficient is indicative of a failure of the passivation film due to wear. The friction durability of the Granocoat 621, DS981LX, and PC-815 passivation films was determined to be 287 s, 581 s and 684 s, respectively, with the water-based polyurethane resin-based passivation film (PC-815) demonstrating superior friction resistance. This enhanced performance is attributed to the strong chemical bonding between the water-based polyurethane and the Al-Zn alloy layer, as well as the synergistic effect of the silane coupling agent. These findings provide both theoretical and experimental foundations for establishing a scientifically validated method for evaluating the friction resistance of Cr-free anti-fingerprint Al-Zn coated carbon steel sheets, offering crucial insights for manufacturers aiming to improve the friction resistance of their products.

**Keywords:** passivation film, hot-dip Al-Zn, carbon steel sheet, friction resistance

Trenutno je še zelo malo znanstvenih raziskav in učinkovitih metodologij s katerimi bi lahko ovrednotili odpornost prevlek proti trenju, ki so namenjene pasivaciji prstnih odtisov, ne vsebujejo Cr in so nanešene na pocinkane jeklene pločevine. To pomembno zmanjšuje kvalitativno oceno in opazovanje (monitoring) kakovosti proizvodov v realnem času, tako proizvajalcev, kot tudi in uporabnikov. V tem članku avtorji predstavljajo sistematično raziskavo odpornosti prevlek brez vsebnosti Cr, nanešenih na pocinkane jeklene pločevine. Cinkanje jeklenih pločevin je bilo predhodno izvedeno z globokim potapljanjem v talin Al-Zn. V raziskavi so uporabili tri glavne tipe pasivacijskih raztopin brez vsebnosti Cr: raztopino na osnovi polimera (Granocoat 621), raztopino na osnovi silana (DS981LX) in raztopino na osnovi smole (PC-815). Za primerjavo so uporabili napravo za ugotavljanje trenja in obrabe na obroču pri visokih hitrostih (angl.: high-speed ring-block friction and wear tester). Eksperimentalni rezultati raziskave so pokazali, da imajo krivulje koeficientov trenja izrazit tristopenjski vzorec, ki se ujema z zaporedjem obrabe pasivacijskega filma, pocinkane Al-Zn plasti in jeklene podlage. Začetno pomembno povečanje koeficienta trenja je posledica odpovedi pasivacijskega filma zaradi obrabe. Ugotovljene trajnosti pasivacijskih prevlek iz Granocoat 621, DS981LX in PC-815 so bile 287 s, 581 s in 684 s. Rezultati so torej pokazali, da ima poliuretanski pasivacijski film na vodni osnovi (PC-815) najboljšo odpornost proti obrabi. To avtorji pripisujejo močni kemijski vezi med polivretanskim filmom in Al-Zn prevleko, kakor tudi sinergijskemu učinku silanskega veziva. Avtorji poudarjajo v zaključkih, da rezultati te teoretične kot tudi eksperimentalne raziskave omogočajo ovrednotenje odpornosti prevlek proti trenju brez Cr za pasivacijo proti prstnim odtisom, ki so nanešene na Al-Zn pocinkanih jeklenih pločevinah. Ta raziskava omogoča tudi kritični vpogled proizvajalcev te vrste izdelkov in njihovo nadaljnje izboljšanje odpornosti proti obrabi.

**Ključne besede:** pasivacijski film (prevleka), globoko potapljanje v talino Al-Zn, pločevina iz ogljičnega jekla, prevleke za pasivacijo prstnih odtisov, odpornost proti trenju

\*Corresponding author's e-mail:  
lzdeyizhang@gmail.com (Deyi Zhang)



© 2025 The Author(s). Except when otherwise noted, articles in this journal are published under the terms and conditions of the Creative Commons Attribution 4.0 International License (CC BY 4.0).

## 1 INTRODUCTION

Hot-dip Al-Zn carbon steel sheets (HDAZSs) are cold-rolled steel sheets coated with an Al-Zn alloy through the hot-dip process. These materials are widely utilized in various applications, including household appliances, consumer electronics, automotive, and electrical equipment.<sup>1</sup> According to a forecast by Global Info Research, the global market value of HDAZSs is projected to reach approximately \$74.6 billion by 2029, with a compound annual growth rate (CAGR) of nearly 2.7 % over the next five years.<sup>2</sup> In response to market demands, the performance evaluation metrics for HDAZSs primarily include corrosion resistance, blackening resistance, yellowing resistance, degreasing resistance, acid resistance, coating adhesion, scratch resistance, and conductivity.<sup>3</sup> To further enhance the performance of HDAZSs and meet the diverse performance requirements of customers, HDAZSs are typically subjected to passivation treatment prior to distribution. Due to environmental concerns, manufacturers predominantly employ organic or organic/inorganic composite passivation processes. The passivation film formed on the surface of an HDAZS effectively prevents corrosive gases and liquids from directly contacting the Al-Zn alloy layer, thereby significantly improving the corrosion resistance, coating adhesion, and acid/alkali resistance.<sup>4,5</sup>

When HDAZSs are employed in household appliances, consumer electronics, food packaging materials, and automotive interior or exterior components that are frequently touched, they are prone to fingerprint contamination, which can negatively impact both aesthetics and user experience. Moreover, oils and sweat residues from fingerprints can serve as breeding grounds for bacteria, thereby compromising the hygiene of the products.<sup>6</sup> As a result, consumer-grade HDAZSs often require excellent anti-fingerprint properties. Currently, the chromium-free (Cr-free) anti-fingerprint passivation solutions available on the market are mainly classified into three categories: polymer-based, resin-based, and silane-based types.<sup>7</sup> Among them, the polymer-based Cr-free anti-fingerprint passivation solution, such as Granocoat 621 from Henkel Corporation (Germany), is widely used by major steel manufacturers in the production of Cr-free anti-fingerprint HDAZS. Resin-based Cr-free passivation solutions are primarily polyurethane-based. One representative example is DS981LX from Wuhan Desytek Environmental Protection & New Materials Co., Ltd. (China), which has demonstrated excellent overall performance in practical applications. Silane-based Cr-free passivation solutions mainly consist of silane coupling agents (e.g., amino sil-

ane and epoxy silane), along with a small amount of nano-SiO<sub>2</sub> modified by silane coupling agents. Commercially available examples include DS981LX from Wuhan Desytek and X220 from Shanghai Xingyu-Ecosil Surface Material Co., Ltd. (China).

This study systematically investigates the friction resistance of hot-dip Al-Zn coated steel sheets (HDAZSs) coated with three types of mainstream Cr-free anti-fingerprint passivation films: Granocoat 621 (polymer-based), DS981LX (silane-based), and PC-815 (resin-based), using a high-speed ring-block friction and wear tester. Under controlled experimental conditions with a fixed speed of 30 rpm and an applied load of 30 N, the friction coefficients of the passivation films exhibit a distinct three-stage pattern, corresponding to the sequential wear of the passivation film, the Al-Zn alloy layer, and the underlying carbon steel substrate. A pronounced initial increase in the friction coefficient serves as a critical indicator of passivation film failure due to wear. By analyzing the time at which this increase occurs, the friction resistance of Cr-free anti-fingerprint HDAZSs can be quantitatively and scientifically assessed. This work contributes to the development of a robust and standardized methodology for evaluating the friction resistance of Cr-free anti-fingerprint HDAZSs, providing manufacturers and end-users with a reliable tool for product quality control. The findings offer important insights for enhancing material durability and performance, thereby advancing quality assurance and product optimization.

## 2 EXPERIMENTAL PART

### 2.1 Materials

Hot-dip Al-Zn coated carbon steel sheets were supplied by the carbon steel sheet factory called Gansu Jiu Steel Group Hongxing Iron & Steel Co., Ltd. (China). The sheets were cut into (50 × 70 × 1) mm specimens using a laser cutting machine (GF4022Plus, Huagong Laser Engineering Co., Ltd., China), leveled with a leveling machine (HPM-60-1600, XUELON Intelligent Equipment Co., Ltd., China), and subsequently subjected to ultrasonic cleaning in acetone for 30 minutes to eliminate surface oils and other contaminants. Following cleaning, the specimens were rinsed with distilled water and dried for subsequent use. The polymer-based Cr-free anti-fingerprint passivation solution (Granocoat 621) was obtained from Henkel Corporation (Germany), the silane-based Cr-free anti-fingerprint passivation solution (DS981LX) was provided by Wuhan Desytek Environmental Protection & New Materials Co., Ltd. (China),

**Table 1:** Compositions and contents of elements in passivation films

Content (mol %)	Fe	C	O	N	Si	P	S	Al	Zn	Na
Granocoat 621	0.749	46.901	16.869	29.398	0.656	0.222	0.458	0.294	4.36	0.094
DS981LX	1.462	44.801	22.716	6.531	21.822	1.584	0.181	0.254	0.774	0.038
PC-815	0.437	55.274	30.801	7.975	3.047	0.865	0.347	0.193	0.982	0.079

and the resin-based Cr-free anti-fingerprint passivation solution (PC-815) was supplied by Hefei Puqing New Material Technology Co., Ltd. (China). The elemental compositions of the passivation films formed by these solutions are detailed in **Table 1**.

## 2.2 Experimental methods

The passivation solutions were uniformly applied to the specimen surfaces using a wire rod coater (4  $\mu\text{m}$ , OSP-04, Japan) and subsequently dried in an oven at 130  $^{\circ}\text{C}$  for 10 min to form chromium-free (Cr-free) anti-fingerprint passivation films. The mass thickness of the resulting passivation films ranged from 1.0  $\text{g}/\text{m}^2$  to 1.2  $\text{g}/\text{m}^2$ , with a physical thickness of approximately 1  $\mu\text{m}$ . The friction resistance of the specimens was evaluated using a high-speed ring-block friction and wear tester (MRH-3A, Jinan Yihua Tribology Testing Technology Co., Ltd., China) under controlled conditions of 30  $\text{min}^{-1}$  and a 30 N load. The friction volume ( $V$ ) and wear rate ( $W$ ) during the friction process were calculated using the following formulas:<sup>8</sup>

$$V = B \times \left[ \frac{\pi R^2}{180} \times \arcsin \left( -\frac{b}{2} \sqrt{R^2 - \frac{b^2}{4}} \right) \right] \quad (1)$$

$$W = \frac{V}{F \times l} \quad (2)$$

where  $V$  is the wear volume ( $\text{mm}^3$ ),  $B$  is the specimen width (mm),  $R$  is the radius of the steel ring (mm),  $b$  is the wear scar width (mm),  $F$  is the load (N),  $L$  is the sliding distance during friction (m), and  $W$  is the wear rate ( $\text{mm}^3/\text{N}\cdot\text{m}$ ). The friction coefficient  $\mu$  was automatically calculated and recorded by the high-speed ring-block friction and wear tester. In accordance with the national standard of China "Artificial Atmosphere Corrosion Test – Salt Spray Test" (GB/T 10125-2012), a 72-hour neutral salt spray corrosion test was conducted on the specimens subjected to varying friction durations to assess their corrosion resistance after different levels of friction-induced damage.

## 2.3 Characterization methods

The surface morphology and three-dimensional (3D) profiles of the specimens following friction and corrosion resistance tests were characterized using metallographic microscopy (Leica, DM2700 M, Germany), laser scanning confocal microscopy (LSCM, Olympus, OLS5000, Japan), and an optical camera (Canon, EOS R7, Japan). Tafel curves and electrochemical impedance spectra (EIS) of the specimens were acquired using an electrochemical workstation (CH Instruments Inc., CHI610, China).

## 3 RESULTS AND DISCUSSION

### 3.1 Friction resistance of Granocoat 621 passivation film

Granocoat 621 is a chromium-free (Cr-free) anti-fingerprint passivation solution developed by Henkel Corporation (Germany) specifically for HDAZSs with exceptional corrosion resistance, humidity resistance, coating adhesion, and anti-fingerprint properties in practical applications. It is widely adopted by leading steel manufacturers. The primary components of Granocoat 621 are a copolymer of vinylpyrrolidone and caprolactam, which bind with the metal surface through van der Waals forces to form a stable film.<sup>3</sup> **Figure 1a** illustrates the friction coefficient curve of the Granocoat 621 passivation film under a load of 30 N and a speed of 30  $\text{min}^{-1}$ . The friction coefficient curve displays a distinct three-stage distribution. In the initial stage (0–287 s), the friction coefficient remains relatively stable, indicating that the passivation film effectively protects the underlying Al–Zn alloy layer during this period. The consistency of the coefficient demonstrates the durability and protective performance of the film under the applied test conditions. In the second stage (287–505 s), the friction coefficient fluctuates significantly, ranging from 0.0065 to 0.0262. The sharp increase at 287 s marks a complete failure of the passivation film, resulting in direct contact between the friction wheel and the Al–Zn alloy surface. These fluctuations are primarily attributed to the non-uniform distribution of residual film fragments generated during the wear process, which intermittently act as localized lubricants. In the third stage (beyond 505 s), the friction coefficient increases sharply again, oscillating between 0.0131 and 0.0585. This significant rise indicates that the Al–Zn alloy layer has been completely worn away, exposing the underlying carbon steel substrate. The pronounced fluctuations in the friction coefficient are primarily attributed to the presence of Al–Zn abrasive dust and residual passivation film debris at the interface between the friction wheel and the carbon steel substrate.

**Figure 1b** shows that the wear rates of the HDAZSs with Granocoat 621 passivation film for friction durations of (200, 400, and 600) s are ( $4.051 \times 10^{-5}$ ,  $7.922 \times 10^{-5}$ , and  $11.485 \times 10^{-5}$ )  $\text{mm}^3/\text{N}\cdot\text{m}$ , respectively. The optical image shown in **Figure 1c** reveals substantial surface darkening in the contact zone. The initial wear analysis after 200 s of testing shows a specimen surface displaying a shallow striated morphology with partial retention of the passivation film integrity. With the increased friction duration of 400 s, the wear tracks develop greater definition, accompanied by emerging regions of metallic luster, indicative of advanced passivation film degradation and incipient wear of the intermediate Al–Zn alloy layer. At the maximum tested duration of 600 s, the wear tracks exhibit fully developed metallic characteristics, providing conclusive evidence of



complete Al-Zn alloy layer penetration and subsequent establishment of direct tribological contact between the carbon steel substrate and friction wheel. After the friction test over 200 s, the surface of the specimen exhibits shallow striated wear patterns with partial preservation of the passivation film. As the friction duration rises to 400 s, the wear tracks become more pronounced, and localized metallic luster can be observed, suggesting near-complete removal of the passivation film and initial wear of the intermediate Al-Zn alloy layer. At the friction duration of 600 s, the wear tracks reveal comprehensive metallic luster, confirming complete wear-through of the Al-Zn alloy layer and subsequent direct interaction between the carbon steel substrate and the friction wheel. Metallographic characterization reveals a well-defined and continuous passivation film network on the HDAZS surface prior to tribological testing (**Figure 1d**), complemented by an LSCM image showing excellent surface uniformity with a small surface height variation of  $3.82\text{ }\mu\text{m}$  (**Figure 1h**).

After the 200-s friction test, distinct striated wear patterns are observed in both metallographic and LSCM images (**Figures 1e** and **1i**). The dark regions in the metallographic image correspond to the residual passivation film, while the bright areas indicate the exposed Al-Zn alloy layer. These striated patterns are visible in the LSCM image. Due to the accumulation of tribological debris, the surface height variation of the specimen reaches  $14.47\text{ }\mu\text{m}$ . After 400-s friction, the wear zone retains its striated morphology but shows a

significant reduction in the dark regions associated with the passivation film. This confirms the penetration of the passivation film and direct contact between the friction wheel and the Al-Zn alloy layer (**Figure 1f**). The LSCM image further reveals partial smoothing of the wear track, with the surface height variation decreasing to  $8.39\text{ }\mu\text{m}$  (**Figure 1j**). When the friction time is extended to 600 s, the wear zone exhibits increased planarity with shallower striations. This is attributed to the higher friction resistance of the underlying carbon steel compared to the passivation film and the intermediate Al-Zn alloy layer, resulting in more uniform wear. In the metallographic image, the dark regions likely correspond to fine particulate debris from the consumed Al-Zn alloy layer, confirming the complete consumption of the Al-Zn alloy layer (**Figure 1g**). The LSCM image reveals a significantly reduced surface topography compared to earlier friction stages, along with a markedly diminished surface height variation relative to the measurements taken after 200 s and 400 s of friction testing (**Figure 1k**).

**Figure 2a** presents Tafel polarization curves of specimens subjected to varying friction durations. The corrosion potential demonstrates a progressive decline with increasing friction time, indicative of frictional damage to the passivation film and consequent reduction in corrosion resistance. Notably, when the friction duration reaches 200 s, the corrosion potential undergoes an abrupt decrease from  $-0.355\text{ V}$  to  $-0.643\text{ V}$ , demonstrating significant degradation of the passivation film during the initial friction phase. As the friction duration extends

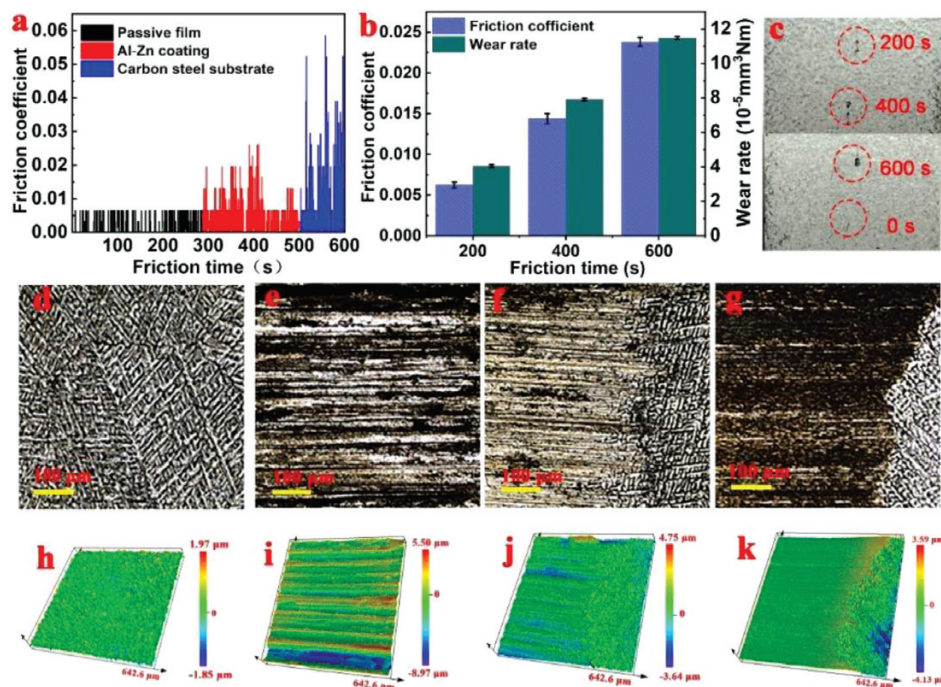


**Figure 1:** a) Friction coefficient curve of the specimens coated with Granocoat 621 passivation film; b) friction coefficients and wear rates of the specimens at different friction times; c) optical images of the specimens after 0, 200, 400, and 600 s of friction testing; d) metallographic images of the specimens after 0 s; e) 200 s; f) 400 s; and g) 600 s of friction testing; h) LSCM images of the specimens after 0 s; i) 200 s; j) 400 s; and k) 600 s of friction testing

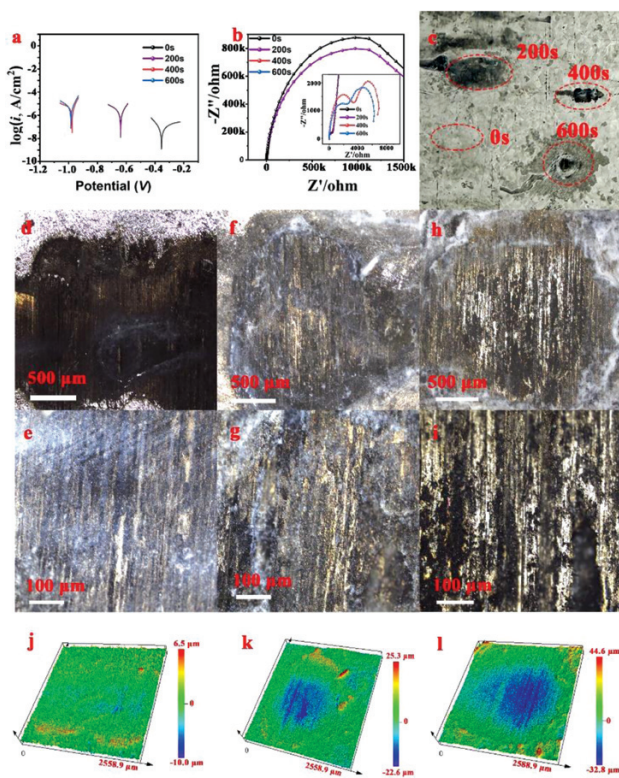


**Figure 2:** a) Tafel polarization curves and b) Nyquist plots, c) of specimens coated with Granocoat 621 passivation film after being subjected to varying friction durations; d), e) optical images of specimens subjected to varying friction durations followed by 72 h salt spray corrosion testing; metallographic images of specimens subjected to 200 s; f), g) 400 s; and h), i) 600 s of friction testing followed by 72 h salt spray corrosion testing; j) laser LSCM images of specimens subjected to 200 s; k) 400 s; and l) 600 s of friction testing followed by 72 h salt spray corrosion testing

from 400 s to 600 s, the corrosion potential shows only a marginal reduction from  $-0.976$  V to  $-0.984$  V, indicating complete wear-through of the passivation film after 400 s of friction, thereby exposing the underlying Al-Zn alloy layer. The EIS analysis of the specimens subjected to varying friction durations further reveals a progressive decrease in polarization resistance with increasing friction time.<sup>9</sup> Particularly, when the friction duration attains 400 s, the polarization resistance experiences a dramatic decline from  $0.287377$  M $\Omega$  to  $11652$   $\Omega$ , approaching the value observed at 600 s of friction testing ( $9434$   $\Omega$ ) (**Figure 2b**). These observations suggest that while the passivation film remains partially intact and continues to provide some degree of protection to the Al-Zn alloy layer at 200 s of friction testing, it loses its protective capability entirely by 400 s of friction testing. Optical images of the specimens subjected to varying friction durations following 72 h of salt spray corrosion testing reveal distinct corrosion characteristics. The specimen subjected to 200 s of friction testing exhibits surface darkening in the friction-affected region without significant pit formation, suggesting partial degradation of the passivation film while maintaining residual protection of the aluminized zinc layer. In contrast, specimens subjected

to 400 s and 600 s of friction testing demonstrate extensive corrosion patterns, indicative of complete passivation film removal and subsequent direct exposure of the substrate to corrosive media (**Figure 2c**). Metallographic analysis after 72 h of salt spray corrosion testing further confirms the corrosion behavior across specimens with varying friction durations. The specimen subjected to 200 s of friction testing exhibits minimal corrosion, with only localized exposure of the metal layer (**Figures 2d** and **2e**). In contrast, specimens subjected to 400 s and 600 s of friction testing display extensive formation of white and black corrosion products, with the specimen subjected to 600 s of friction testing demonstrating particularly severe corrosion damage (**Figures 2f–2i**). These observations align with the progressive degradation of the passivation film and increased susceptibility to corrosion with extended friction duration (**Figures 2j–2l**). LSCM images of the specimen subjected to varying friction durations following 72 h of salt spray corrosion testing reveal distinct surface topography characteristics. The specimen subjected to 200 s of friction maintains a relatively flat surface morphology, exhibiting a minimal height difference of only  $16.5$   $\mu\text{m}$ . In contrast, specimens subjected to 400 s and 600 s of friction demonstrate a significant increase in surface roughness, accompanied by the formation of prominent corrosion pits.

### 3.2 Friction resistance evaluation of DS981LX passivation film

DS981LX is a Cr-free anti-fingerprint passivation solution developed by Wuhan Desytek Environmental Protection & New Materials Co., Ltd. (China), utilizing silane coupling agents as its primary components. To enhance both corrosion resistance and friction resistance, a small quantity of silane coupling agent-modified nano-SiO<sub>2</sub> is incorporated into the solution. The friction coefficient of the HDAZSs coated with the DS981LX passivation film demonstrates a three-stage distribution, corresponding to the sequential friction of the passivation film, the hot-dip Al-Zn alloy layer, and the underlying carbon steel substrate, respectively (**Figure 3a**). In comparison to the Granocoat 621 passivation film, the DS981LX passivation film exhibits significantly enhanced friction durability, extending to 581 s, while maintaining a comparable friction coefficient of 0.0063. Granocoat 621 primarily consists of a copolymer of vinylpyrrolidone and caprolactam, which forms a stable film on a metal surface through van der Waals forces, resulting in a relatively weak interaction between the passivation layer and the Al-Zn alloy layer. In contrast, DS981LX is primarily composed of silane coupling agents, whose molecular structure contains silicon-oxygen bonds capable of forming strong chemical bonds with the Al-Zn alloy layer surface,<sup>5</sup> thereby improving its friction resistance.



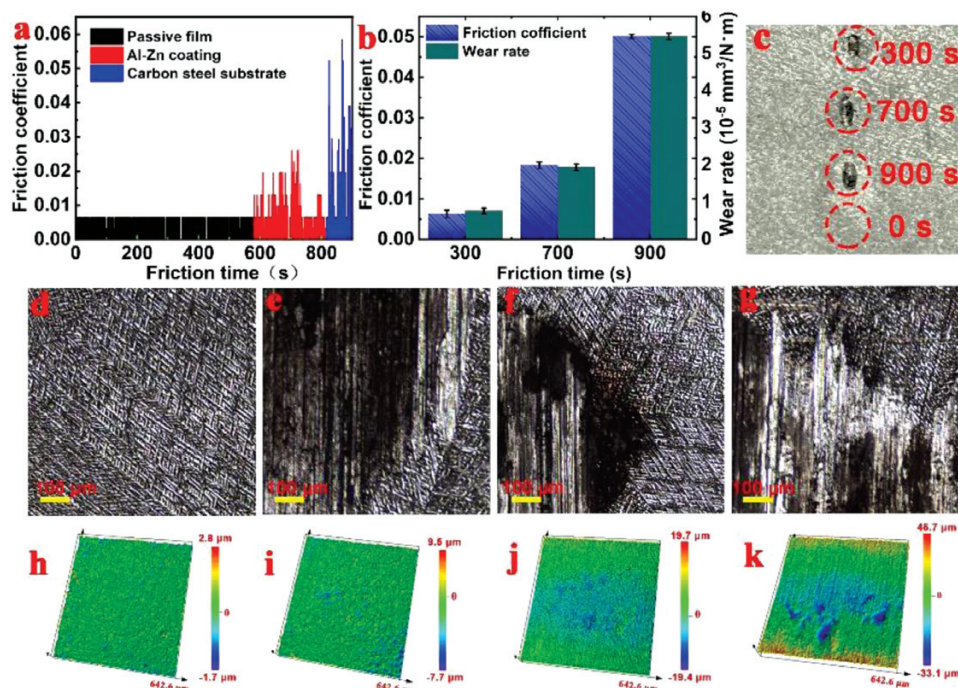


**Figure 3:** a) Friction coefficient curve of the specimens coated with DS981LX passivation film; b) friction coefficient and wear rate of the specimens at different friction times; c) optical images of the specimens after 0 s, 300 s, 700 s, and 900 s of friction testing; metallographic images of the specimens after d) 0 s, e) 300 s, f) 700 s, and g) 900 s of friction testing; LSCM images of the specimens after h) 0 s, i) 300 s, j) 700 s, and k) 900 s of friction testing

Furthermore, DS981LX incorporates silane coupling agent-modified nano-SiO<sub>2</sub>, which migrates to the friction interface during testing, forming a uniform lubricating film that further enhances the friction resistance of the passivation film. Compared to the Granocoat 621 passivation film, the friction durability of the DS981LX passivation film is significantly extended to 581 s, with a friction coefficient of 0.0063, similar to that of Granocoat 621. When the friction duration reaches 581–819 s, the friction coefficient exhibits a sudden increase, signifying that the DS981LX passivation film has been completely worn away, thereby losing its protective effect on the Al-Zn alloy layer. Consequently, the friction wheel begins to directly abrade the surface of the Al-Zn alloy layer. Upon exceeding 819 s, the friction coefficient rises once more, which correlates with the complete wear-through of the Al-Zn alloy layer, leading to the initiation of friction against the underlying carbon steel substrate. The wear rates of the DS981LX passivation film at friction durations of 300, 700, and 900 s are  $0.769 \times 10^{-5}$ ,  $1.919 \times 10^{-5}$ , and  $5.847 \times 10^{-5} \text{ mm}^3/\text{N}\cdot\text{m}$ , respectively (Figure 3b). The comparatively lower wear rate relative to the Granocoat 621 passivation film is identified as the primary factor contributing to its superior friction durability. Optical images captured before and after friction testing reveal that the friction-affected area darkens after (300, 700, and 900) s of friction. However, after 300 s of friction, the wear tracks still exhibit the presence of a continuous passivation film, indicating that the film has

not been entirely worn through and continues to provide protection to the Al-Zn alloy layer (Figure 3c).

Metallographic images before and after friction testing clearly demonstrate that after 300 s of friction, the passivation film is partially damaged, with only a minimal portion of the Al-Zn alloy layer exposed. Following 700 s of friction, the passivation film is nearly entirely degraded, resulting in significant exposure of the Al-Zn alloy layer. After 900 s of friction, the friction-affected region exhibits a bright metallic luster, confirming that the Al-Zn alloy layer has been completely worn through, thereby exposing the underlying carbon steel substrate (Figures 3d–3g). LSCM images further reveal that as friction duration increases, the wear tracks become increasingly pronounced (Figures 3h–3k). After 300 s of friction, the blue regions in the LSCM images, corresponding to friction-induced pits, occupy a relatively small area, indicating that the passivation film has not yet delaminated from the Al-Zn alloy layer. However, the height difference between the lowest and highest points on the specimen surface reaches 17.2  $\mu\text{m}$ , with the deepest wear track measuring 7.7  $\mu\text{m}$ , confirming partial degradation of the passivation film. After 700 s of friction, the blue area expands significantly, and the surface height difference increases to 39.1  $\mu\text{m}$ , suggesting substantial delamination of the passivation film from the specimen surface, rendering it ineffective in protecting the Al-Zn alloy layer. By 900 s of friction, both the area and depth of the friction pits continue to grow, indicating

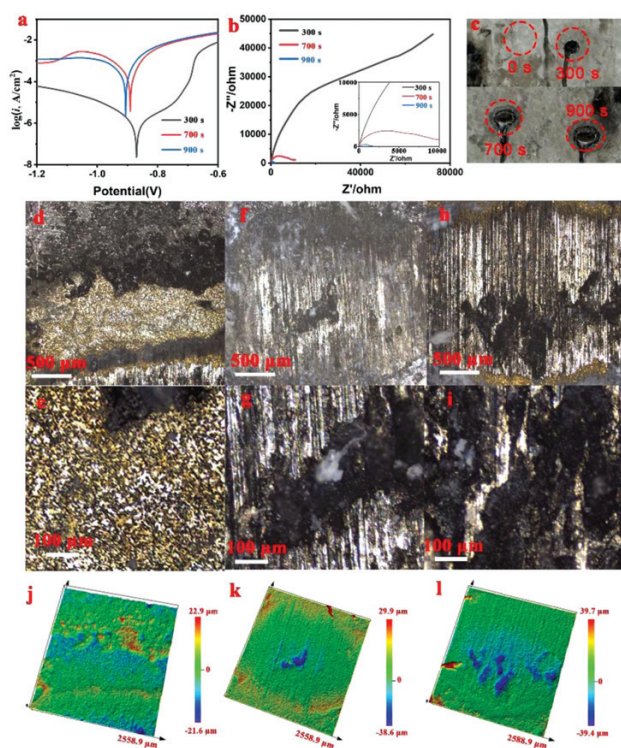


**Figure 4:** a) Tafel polarization curves and b) Nyquist plots of specimens coated with DS981LX passivation film after being subjected to varying friction durations; optical images of specimens subjected to varying friction durations followed by 72 h salt spray corrosion testing; metallographic images of specimens subjected to d), e) 300 s, f), g) 700 s, and h), i) 900 s of friction testing followed by 72 h salt spray corrosion testing; laser LSCM images of specimens subjected to j) 300 s, k) 700 s, and l) 900 s of friction testing followed by 72 h salt spray corrosion testing

severe damage to the aluminized zinc layer and the onset of wear on the underlying carbon steel substrate.

**Figure 4a** presents Tafel polarization curves of the HDAZS specimens coated with the DS981LX passivation film after varying friction durations. As the friction time increases from 300 to 700 s, the corrosion potential of the specimen shifts from  $-0.875$  to  $-0.891$  V, while the corrosion current density rises sharply from  $1.112 \times 10^{-6}$  to  $9.425 \times 10^{-4}$  A/cm<sup>2</sup>, indicating a rapid deterioration in the specimen's corrosion resistance with prolonged friction. This behavior is attributed to the fact that after 300 s, the passivation film remains partially intact, continuing to provide some degree of protection to the Al-Zn alloy layer. However, after 700 s, the Al-Zn alloy layer is fully exposed, and the absence of the passivation film leads to a significant reduction in corrosion resistance. After 900 s, the corrosion potential further decreases to  $-0.906$  V, signifying an additional decline in corrosion resistance. EIS results reveal that after (300, 700, 900) s of friction testing, the polarization resistances are (20766.8, 6234.6, and 1320.8)  $\Omega$ , respectively (**Figure 4b**). The substantial reduction in polarization resistance as the friction time increases from (300 to 700) s confirms the near-complete loss of the passivation film's

protective effect on the Al-Zn alloy layer, indicating that the passivation film has been entirely worn through. Optical images obtained after 72 h of salt spray corrosion reveal that the friction-affected area of the specimen subjected to 300 s of friction exhibits a blackened appearance but no distinct corrosion pits. In contrast, specimens subjected to 700 s and 900 s of friction display pronounced corrosion pits and white corrosion products (**Figure 4c**). Metallographic images further demonstrate that the specimen subjected to 300 s of friction exhibits numerous localized pitting corrosion sites but no extensive general corrosion, suggesting that the passivation film retains partial protection over the specimen surface. Specimens subjected to 700 s and 900 s of friction, however, exhibit extensive general corrosion, with both the corrosion area and depth increasing proportionally with friction duration (**Figures 4d–4i**). LSCM images corroborate these findings, showing that after 72 h of salt spray corrosion, the specimen subjected to 300 s of friction does not exhibit general corrosion, but a height difference of 44.  $\mu\text{m}$ . In contrast, specimens subjected to 700 s and 900 s of friction display significant general corrosion, with height differences of 68.5  $\mu\text{m}$  and 79.1  $\mu\text{m}$ , respectively. These results confirm that the residual passivation film after 300 s of friction continues to provide a degree of protection to the specimen surface.

### 3.3 Friction resistance evaluation of PC-815 passivation film

PC-815 passivation solution, manufactured by Hefei Puqing New Material Technology Co., Ltd., is a Cr-free anti-fingerprint passivation solution primarily composed of water-based anionic polyurethane resin, with a minor addition of silane coupling agent. Similar to Granocoat 621 and DS981LX passivation films, the friction coefficient of the PC-815 passivation film demonstrates a triphasic distribution as a function of friction time (**Figure 5a**). Notably, the friction coefficient exhibits transitions at 684 s and 862 s, revealing that the friction durability of the PC-815 passivation film extends to 684 s, surpassing that of Granocoat 621 and DS981LX. Within the friction time interval of 0–684 s, the friction coefficient of PC-815 passivation film oscillates between 0.0054 and 0.0123, with an average friction coefficient of 0.0089, which is superior to those of Granocoat 621 and DS981LX (**Figure 5b**). At a friction time of 350 s, the wear rate of PC-815 is merely 0.232 mm<sup>3</sup>/N·m, substantially lower than those of Granocoat 621 and DS981LX passivation films. The robust chemical interaction between the water-based polyurethane resin and the Al-Zn alloy layer,<sup>10,11</sup> combined with the synergistic effect of silane coupling agent, underpins the exceptional friction resistance of the PC-815 passivation film. **Figure 5c** presents optical images of the PC-815 passivation film subjected to varying friction durations. After 350 s of friction, the wear patterns are manifested as striations, with minimal exposure of the Al-Zn alloy layer, indicat-



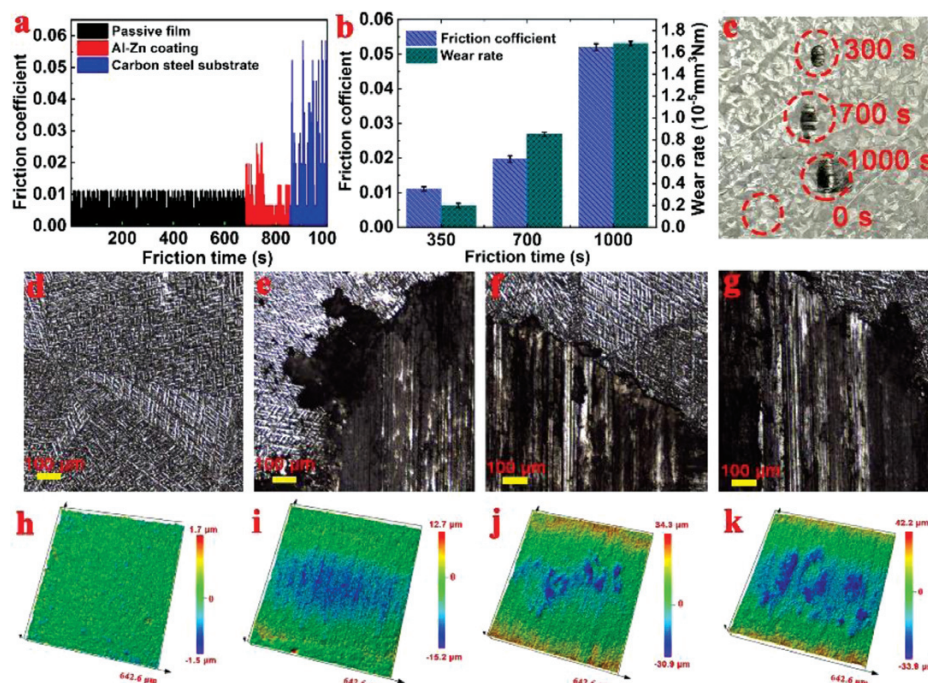


**Figure 5:** a) Friction coefficient curve of the specimens coated with PC-815 passivation film; b) friction coefficient and wear rate of the specimens at different friction times; c) optical images of the specimens after 0, 350, 700, and 900 s of friction testing; metallographic images of the specimens after d) 0 s; e) 350 s; f) 700 s and g) 900 s of friction testing; LSCM images of the specimens after h) 0 s; i) 350 s; j) 700 s; and k) 900 s of friction testing

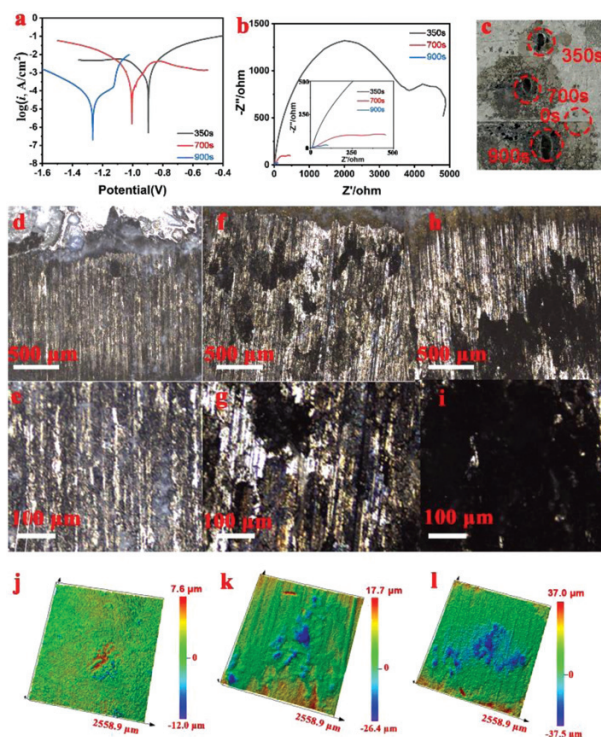


**Figure 6:** a) Tafel polarization curves and b) Nyquist plots of specimens coated with PC-815 passivation film after being subjected to varying friction durations; c) optical images of specimens subjected to varying friction durations followed by 72 h salt spray corrosion testing; metallographic images of specimens subjected to d) 300 s; e) 500 s; f) 700 s; and g) 900 s of friction testing followed by 72 h salt spray corrosion testing; LSCM images of specimens subjected to j) 300 s; k) 700 s; and l) 900 s of friction followed by 72 h salt spray corrosion testing

ing that the passivation film remains partially intact and continues to provide protection to the underlying Al-Zn alloy layer. At friction durations of 700 s and 900 s, the wear patterns broaden, revealing extensive areas of silver-white metal. After 900 s of friction, the entire contact region between the specimen and the friction wheel exhibits a silver-white hue. Metallographic images obtained at different friction intervals corroborate that after 350 s of friction, the passivation film is not entirely abraded, with only slight exposure of the Al-Zn alloy layer. However, after 700 s and 900 s of friction, the passivation film ceases to protect the metal layer effectively (**Figures 5d–5g**). LSCM images reveal that after 350 s of friction, the specimen surface displays striated wear patterns, with groove-like wear marks (blue regions) interspersed with residual passivation film (green regions). Subsequent to 700 s and 900 s of friction, the wear patterns evolve into flake-like formations, and the depth of these wear marks progressively increases with prolonged friction time (**Figures 5h–5k**).

Tafel polarization curves of the specimen coated with the PC-815 passivation film subjected to varying friction durations reveal a progressive decline in corrosion resistance with increasing friction time. As the friction time escalates from 350 s to 700 s, the corrosion potential of the specimen shifts from  $-0.895$  to  $-1.005$  V, accompanied by a marked surge in corrosion current density from  $1.432 \times 10^{-6}$  to  $5.426 \times 10^{-4}$  A/cm<sup>2</sup> (**Figure 6a**). EIS spectra measurements further demonstrate that the polarization resistances are (29844.6, 5348.2, and 852.4)  $\Omega$  after



(350, 700, and 900) s of friction, respectively. A significant reduction in polarization resistance is observed as the friction time increases from 350 s to 700 s (**Figure 6b**). Optical images taken after 72 h of salt spray corrosion indicate that the friction-affected regions darken; however, the specimen subjected to 350 s of friction exhibits no conspicuous corrosion pits or accumulation of corrosion products. In contrast, specimens subjected to 700 s and 900 s of friction display pronounced corrosion pits and white corrosion products (**Figure 6c**). Metallographic images corroborate that the specimen subjected to 350 s of friction primarily undergoes pitting corrosion, with no evidence of extensive uniform corrosion. Conversely, specimens subjected to 700 s and 900 s of friction exhibit widespread uniform corrosion, with both the area and depth of corrosion escalating with prolonged friction time (**Figures 6d–6i**). LSCM images further substantiate that, following 72 h of salt spray corrosion, the specimen subjected to 350 s of friction does not exhibit significant uniform corrosion, whereas those subjected to 700 s and 900 s of friction are severely compromised by corrosion (**Figures 6j–6l**).

The above results demonstrate that a high-speed ring-block friction and wear tester enables systematic monitoring of variations in the friction coefficient on a specimen surface. The abrupt changes observed in the friction coefficient signify transitions in the friction interfaces, thereby offering a scientific foundation for evaluating the friction resistance of chromium-free anti-fingerprint aluminized zinc steel sheets.

#### 4 CONCLUSIONS

Friction tests were conducted on HDAZSs coated with polymer-based (Granocoat 621), silane-based (DS981LX), or resin-based (PC-815) passivation films using a high-speed ring-block friction and wear tester. The resulting friction coefficient curves display a distinct triphasic pattern, corresponding sequentially to the wear of the passivation film, the underlying Al–Zn alloy layer, and finally the carbon steel substrate. The initial marked increase in the friction coefficient signifies a complete failure of the passivation film due to wear. By identifying the time at which this increase occurs, a quantitative evaluation of the friction resistance of each Cr-free anti-fingerprint HDAZS can be established. The friction durability of Granocoat 621, DS981LX, and PC-815 passivation films is determined to be 287 s, 581 s, and 684 s, respectively. Among them, the water-based polyurethane resin-based PC-815 demonstrated the highest friction resistance. This superior performance is primar-

ily attributed to the strong chemical bonding between the polyurethane matrix and the Al–Zn alloy layer, as well as the synergistic effect provided by the incorporated silane coupling agent.

#### Acknowledgment

This work was supported by the Science and Technology Major Project of Gansu, China (Grant No. 22ZD6GB019).

#### 5 REFERENCES

- J. K. Chang, C. S. Lin, W. R. Wang, S.-Y. Jian, High temperature deformation behaviors of hot dip 55 wt% Al–Zn coated steel, *App. Surf. Sci.*, 511 (2020), 145550, doi:10.1016/j.apsusc.2020.145550
- J. Li, Z. Zhao, X. Tang, Y. Wang, Y. Cao, Y. Li, X. Yuan, D. Zhang, The effect of a Cr-free fingerprint-resistant passivation film on the performance of hot-dip 55% Al–Zn coated steel, *Mater. Tehnol.*, 58 (2024), 511–520, doi:10.17222/mit.2024.1160
- D. Qiao, J. Li, X. Tang, Y. Shi, Y. Wang, Y. Cao, Z. Zhang, Y. Li, X. Yuan, D. Zhang, The effect of yellowing on the corrosion resistance of chromium-free fingerprint-resistant hot-dip Al–Zn-coated steel, *Processes*, 13 (2025), 351, doi:10.3390/pr13020351
- C. F. Glover, R. Subramanian, G. Williams, In-coating phenyl phosphonic acid as an etch-primer corrosion inhibitor system for hot dip galvanized steel, *J. Electrochem. Soc.*, 162 (2015), C433, doi:10.1149/2.0191509jes
- Z. X. Liu, L. Shi, A. Y. Jiang, J. X. Liu, B. F. Zhang, Y. J. Zhou, G. P. Zhang, Corrosion protection investigations of oxide-silane composite coating on hot dip aluminized steel, *Mater. Corros.*, 76 (2025), 87–98, doi:10.1002/maco.202414506
- G. Yang, Z. Zhang, C. Li, J. Hu, A facile approach to fabricate omniphobic and robust polyurethane coatings for anti-smudge, anti-ink, *Prog. Org. Coat.*, 179 (2023), 107488, doi:10.1016/j.porgcoat.2023.107488
- Z. Yu, J. Hu, H. Meng, A review of recent developments in coating systems for hot-dip galvanized steel, *Front. Mater.*, 7 (2020) 74, doi:10.3389/fmats.2020.00074
- S. Boopathi, M. Jeyakumar, G. R. Singh, F. L. King, M. Pandian, R. Subbiah, V. Haribalaji, An experimental study on friction stir processing of aluminium alloy (AA-2024) and boron nitride (BNp) surface composite, *Mater. Today: Proc.*, 59 (2022), 1094–1099, doi:10.1016/j.matpr.2022.02.435
- A. Chaouki, S. C. Cifuentes, J. Bedmar, J. Rams, K. El Maalam, K. Aouadi, S. Naamane, I. Benabdallah, A. El Fatimy, M. B. Ali, Investigation of coating weight and steel substrate on the properties of hot-dip galvanized coatings, *Sur. Coat. Tech.*, 497 (2025), 131804, doi:10.1016/j.surfcoat.2025.131804
- M. Yadav, J. K. Saha, S. K. Ghosh, Surface, chemical, and mechanical properties of polyurethane-coated galvanized steel sheets, *J. Mater. Engin. Perform.*, 34 (2025), 1177–1192, doi:10.1007/s11665-024-09171-6
- S. Zafar, R. Kahraman, R. A. Shakoor, Recent developments and future prospective of polyurethane coatings for corrosion protection – a focused review, *Eur. Polym. J.*, 220 (2024), 113421, doi:10.1016/j.eurpolymj.2024.113421